Implementation of a Near-Field to Far-Field Transformation to Calculate Far Fields of Radiating Objects.

Erich Wanzek

ELEC 4333, University of Colorado Denver

(Dated: May 14, 2021)

I. PROJECT DESCRIPTION

The objective of this project was to develop a script in MATLAB that performs a near-field to far-field transformation near fields produced in the FDTD simulation. When performing a FDTD simulation, the number of cells in the simulation volume must be limited in order for the simulation not to become computationally intensive. This poses as problem, however, if it is desired to analyze the fields far away from scattering or radiating object since this would require very computational intensive FDTD simulations to extend the FDTD grid out to far distances. To solve this issue, it is necessary to perform a Near-Field to Far-Field transformation (NFFF). The NFFF can predict the electromagnetic fields anywhere outside the FDTD simulation volume by only the information of the tangential fields present on a closed hypothetical surface, called the Huygens surface, that bounds the device under test in FDTD simulation volume.

In this project a MATLAB script will be integrated into a provided FDTD software package authored by Dr. Gedney. The project goal is to use the implemented NFFF to calculate the radiation gain pattern of an antenna such as a dipole antenna. This can be accomplished by simulating the antenna in a FDTD volume with a Huygens surface that bounds the Antenna. The Huygens surface is a hypothetical surface on which the tangential electric and magnetic fields are measured in order to calculate the magnetic and electric currents surface destines to solve for the electric and magnetic vector potentials outside the volume bounded by the Huygens surface. After the electromagnetic transients pass through the Huygens surface the propagating electromagnetic energy and any evanescent electromagnetic fields will be absorbed by a perfectly match layer. Figure 1 shows the general FDTD setup for this project.

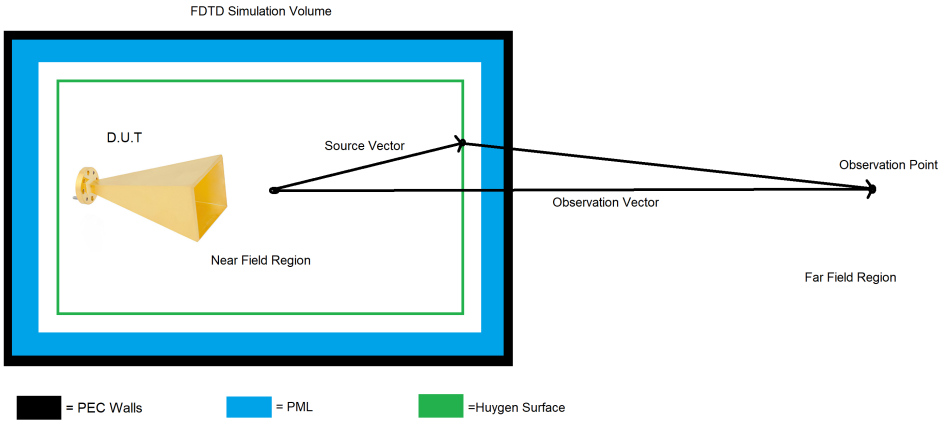

FIG. 1: Illustration of the necessity and implementation of a a Near to far field transformation for a FDTD simulation of a Horn Antenna. In order to predict the fields in the far field region which lie far outside the FDTD simulation Volume, a Huygens surface is situated in the FDTD space before the PML, on which the tangential field components are sampled in order to predict fields in the far field.

The Near-Field to Far-Field transform MATLAB script will be verified with the simulation case of simple Hertzian dipole. If the verification process is achieved, the code will be used calculate the antenna radiation pattern of the square dipole antenna provided in the file.

II. THEORY

The Near-Field to Far Field (NFFF) transform is accomplished by using the surface equivalence principle, Green's second identity and electromagnetic potential theory. The surface equivalent principles states that radiating fields produced from magnetic and electric current densities in the volume bounded by the Huygens surface are equivalent to radiating fields produced from surface magnetic and electric currents on the Huygens surface that were produce from the bounded volume currents. Using vector potential theory, the electric and magnetic fields can be formulated in terms of vector potential fields. The electric and magnetic vector potentials can be calculated from the magnetic and electric current densities and this relates to Green's second identity which states that if the tangential fields on a closed surface are known, then the fields exterior to the Huygens surface can be uniquely calculated

from solely the knowledge of the surface tangential fields.

Using the formulation of electromagnetic potentials, the electric and magnetic fields can be formulated in terms of the vector potentials in the frequency domain given by:

$$\vec{E}(\vec{r}) = -j\omega\mu(\vec{r}) + \frac{1}{j\omega\varepsilon}\nabla\nabla\cdot\vec{A}(\vec{r}) - \nabla\times\vec{F}(\vec{r}) \tag{1}$$

$$\vec{H}(\vec{r}) = -j\omega\varepsilon(\vec{r}) + \frac{1}{j\omega\mu}\nabla\nabla\cdot\vec{F}(\vec{r}) - \nabla\times\vec{A}(\vec{r}) \tag{2}$$

.

In these equations, A is the magnetic vector potential, and F is the electric vector potential. The magnetic and electric vector potentials can be calculated by a spatial convolution of the magnetic and current densities with a spherical wave of spatial frequency in the time domain as defined by the equations:

$$\vec{A}(\vec{r}) = \iiint_V \vec{J}^i(\vec{r})\frac{e^{-jkR}}{4\pi R}dv' \tag{3}$$

$$\vec{F}(\vec{r}) = \iiint_V \vec{M}^i(\vec{r})\frac{e^{-jkR}}{4\pi R}dv' \tag{4}$$

.

In these equations, r' represents the source coordinate vector and r represents the observation coordinate vector and R represent the distance vector between the two vectors defined as R=—r-r—. K is the wave number, which is different for every frequency that the vector potentials need to be calculated at for every time harmonic of the electric and magnetic currents.

If a hypothetical closed surface, called the Huygens surface, now bounds the time harmonic magnetic and electric volume current densities, current densities on the surface can now be defined from the tangential electric and magnetic fields present on the Huygens surface as:

$$\overrightarrow{J_s}(\overrightarrow{r_s}) = \widehat{n}\times\overrightarrow{H}(\overrightarrow{r_s}) \tag{5}$$

$$\overrightarrow{M_s}(\overrightarrow{r_s}) = \widehat{n}\times\overrightarrow{E}(\overrightarrow{r_s}) \tag{6}$$

.

According to the surface equivalence principle, these hypothetical surface current densities originating from volume current densities will radiate the same fields that would be radiated form the volume current densities bounded by the surface. With the Huygens surface in place, Green's second identity states that with just the information of the tangential fields on the closed Huygens surface, all fields exterior to the surface can be uniquely predicted. Using the surface equivalence principle and Green's second identify, the vector potentials for predicting the far fields can now be defined in terms of the equivalent surface densities on the Huygens surface as:

$$\vec{A}(\vec{r}) = \iint_S \vec{J}_s(\vec{r}) \frac{e^{-jkR}}{4\pi R} ds' \tag{7}$$

$$\vec{F}(\vec{r}) = \iint_S \vec{M}_s(\vec{r}) \frac{e^{-jkR}}{4\pi R} ds' \tag{8}$$

.

With the vector potentials now defined only from the surface current densities derived from the tangential field information on the surface, all fields can now be computed outside this surface. In the FDTD field simulation, the Huygens surface surface in defined as a rectangular surface coinciding with the FDTD lattice. This allows the tangential electric and magnetic fields of the Huygens surface to simply be the electric fields of the primary grid edges coinciding with the defined surface and a averaged magnetic filed o the secondary grid corresponding the primary grid coinciding with the defined Huygens surface. These tangential field of the FDTD lattice coinciding with the defined rectangular Huygens surface are sampled at each time step and used to calculate the far fields for any location outside the FDTD space by use of equation 7 and 8. The difference in the source vector to the observation vector point is defined as:

$$R = |\overrightarrow{r} - \overrightarrow{r'}| = \sqrt{r^2 + r'^2 - 2rr'(\widehat{r} \cdot \widehat{r'})}. \tag{9}$$

. In the far field approximation this is approximated as:

$$R \approx r - r \cdot r' \approx r - r' \cos \Psi \tag{10}$$

.

Using equations 7 and 8 and the far field approximation, the vector potential equations 1 and 2 can be applied to calculate the far-field electric and magnetic fields. Doing this in

spherical coordinates results in the electric and magnetic fields defined in spherical vectors as:

$$E_r \approx 0 \tag{11}$$

$$E_\theta \approx -jk\frac{e^{-jkr}}{4\pi r}(L_\phi + \eta N_\theta) \tag{12}$$

$$E_\phi \approx jk\frac{e^{-jkr}}{4\pi r}(L_\theta - \eta N_\phi) \tag{13}$$

$$H_r \approx 0 \tag{14}$$

$$H_\theta \approx jk\frac{e^{-jkr}}{4\pi r}(N_\phi - \frac{1}{\eta}N_\theta) = -\frac{1}{\eta}E_\phi \tag{15}$$

$$H_\phi \approx -jk\frac{e^{-jkr}}{4\pi r}(N_\theta + \frac{1}{\eta}N_\phi) = \frac{1}{\eta}E_\theta \tag{16}$$

. In theses equations N and L are given by the expressions:

$$\overrightarrow{N}(\theta,\phi) \approx \int_S \overrightarrow{J_s}(f,\overrightarrow{r'})e^{j\overrightarrow{k}\cdot\overrightarrow{r'}}ds'; \tag{17}$$

$$\overrightarrow{L}(\theta,\phi) \approx \int_S \overrightarrow{M_s}(f,\overrightarrow{r'})e^{j\overrightarrow{k}\cdot\overrightarrow{r'}}ds'; \tag{18}$$

,

where, $\vec{r'}$ is the position vector to source point on the Huygen surface and k is the wave vector to the observation point. The wave vector to the observation point is given as:

$$\vec{k} = k\hat{r} = k(\sin\theta\cos\phi\hat{x} + \sin\theta\sin\phi\hat{y} + \cos\theta\hat{z}) \tag{19}$$

.

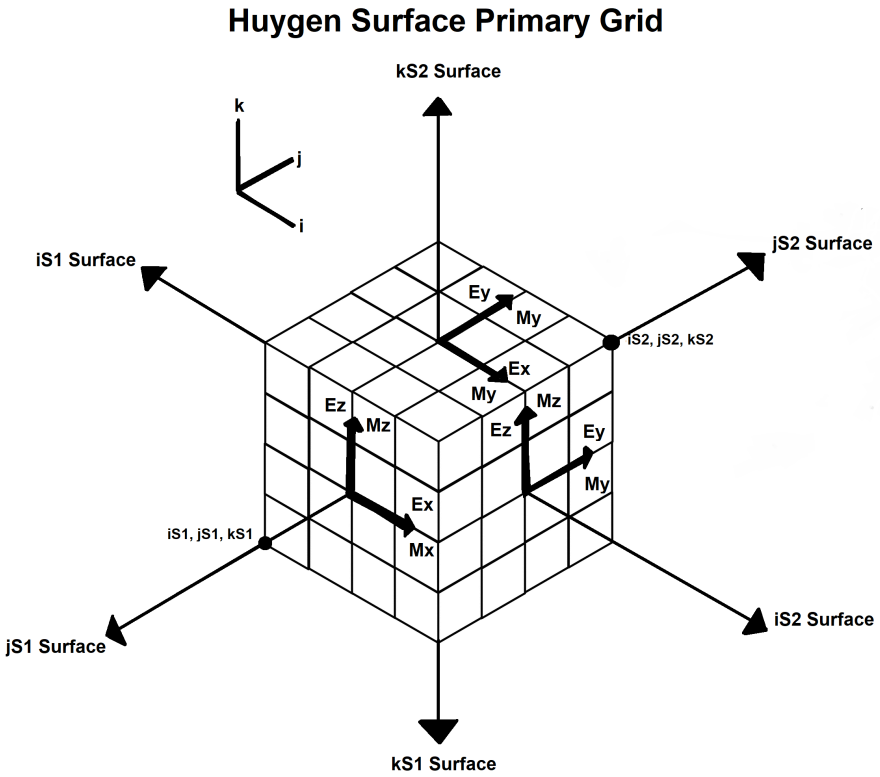

FIG. 2: Illustration of the Huygens surface as defined on the primary grid. There are six surfaces that form the Rectangular Huygens surface in the 3d FDTD lattice. For each surface the magnetic currents orthogonal to the surface normal vector are expressed in terms of the tangential electric fields on that surface.

The magnetic current densities are defined on the Huygens surface by applying EQ.6 on all the tangential electric fields on the primary grid of the FDTD lattice that coincide with the defined Huygens surface. The derived magnetic surface current densities for each of the six faces of the Huygens surface are defined by the normal surface vector labeled is1,js1,ks1,is2,js2,ks2 as illustrated in FIG 2. The magnetic surface current densities are related to the tangential electric fields as given by the relations:

$$\vec{M}\ on\ is1 \begin{cases} \hat{z}M^{n+\frac{1}{2}}_{z_{is1,j+\frac{1}{2},k}} = \hat{y}E^{n+\frac{1}{2}}_{y_{is1,j+\frac{1}{2},k}} \times -\hat{x} = \quad \hat{z}E^{n+\frac{1}{2}}_{y_{is1,j+\frac{1}{2},k}} \\ \hat{y}M^{n+\frac{1}{2}}_{y_{is1,j,k+\frac{1}{2}}} = \hat{z}E^{n+\frac{1}{2}}_{z_{is1,j,k+\frac{1}{2}}} \times -\hat{x} = -\hat{y}E^{n+\frac{1}{2}}_{z_{is1,j,k+\frac{1}{2}}} \end{cases} \tag{20}$$

$$\vec{M}\ on\ js1 \begin{cases} \hat{x}M^{n+\frac{1}{2}}_{x_{i,js1,k+\frac{1}{2}}} = \hat{z}E^{n+\frac{1}{2}}_{z_{i,js1,k+\frac{1}{2}}} \times -\hat{y} = \quad \hat{x}E^{n+\frac{1}{2}}_{z_{i,js1,k+\frac{1}{2}}} \\ \hat{z}M^{n+\frac{1}{2}}_{z_{i+\frac{1}{2},js1,k}} = \hat{x}E^{n+\frac{1}{2}}_{x_{i+\frac{1}{2},js1,k}} \times -\hat{y} = -\hat{z}E^{n+\frac{1}{2}}_{x_{i+\frac{1}{2},js1,k}} \end{cases} \tag{21}$$

$$\vec{M}\ on\ ks1 \begin{cases} \hat{y}M^{n+\frac{1}{2}}_{y_{i+\frac{1}{2},j,ks1}} = \hat{x}E^{n+\frac{1}{2}}_{x_{i+\frac{1}{2},j,ks1}} \times -\hat{z} = \quad \hat{y}E^{n+\frac{1}{2}}_{x_{i+\frac{1}{2},j,ks1}} \\ \hat{x}M^{n+\frac{1}{2}}_{x_{i,j+\frac{1}{2},ks1}} = \hat{y}E^{n+\frac{1}{2}}_{y_{i,j+\frac{1}{2},ks1}} \times -\hat{z} = -\hat{x}E^{n+\frac{1}{2}}_{y_{i,j+\frac{1}{2},ks1}} \end{cases} \tag{22}$$

$$\vec{M}\ on\ is2 \begin{cases} \hat{z}M^{n+\frac{1}{2}}_{z_{is2,j+\frac{1}{2},k}} = \hat{y}E^{n+\frac{1}{2}}_{y_{is2,j+\frac{1}{2},k}} \times \hat{x} = -\hat{z}E^{n+\frac{1}{2}}_{y_{is2,j+\frac{1}{2},k}} \\ \hat{y}M^{n+\frac{1}{2}}_{y_{is2,j,k+\frac{1}{2}}} = \hat{z}E^{n+\frac{1}{2}}_{z_{is2,j,k+\frac{1}{2}}} \times \hat{x} = \quad \hat{y}E^{n+\frac{1}{2}}_{z_{is2,j,k+\frac{1}{2}}} \end{cases} \tag{23}$$

$$\vec{M}\ on\ js2 \begin{cases} \hat{x}M^{n+\frac{1}{2}}_{x_{i,js2,k+\frac{1}{2}}} = \hat{z}E^{n+\frac{1}{2}}_{z_{i,js2,k+\frac{1}{2}}} \times \hat{y} = -\hat{x}E^{n+\frac{1}{2}}_{z_{i,js2,k+\frac{1}{2}}} \\ \hat{z}M^{n+\frac{1}{2}}_{z_{i+\frac{1}{2},js2,k}} = \hat{x}E^{n+\frac{1}{2}}_{x_{i+\frac{1}{2},js2,k}} \times \hat{y} = \quad \hat{z}E^{n+\frac{1}{2}}_{x_{i+\frac{1}{2},js2,k}} \end{cases} \tag{24}$$

$$\vec{M}\ on\ ks2 \begin{cases} \hat{y}M^{n+\frac{1}{2}}_{y_{i+\frac{1}{2},j,ks2}} = \hat{x}E^{n+\frac{1}{2}}_{x_{i+\frac{1}{2},j,ks2}} \times \hat{z} = -\hat{y}E^{n+\frac{1}{2}}_{x_{i+\frac{1}{2},j,ks2}} \\ \hat{x}M^{n+\frac{1}{2}}_{x_{i,j+\frac{1}{2},ks2}} = \hat{y}E^{n+\frac{1}{2}}_{y_{i,j+\frac{1}{2},ks2}} \times \hat{z} = \quad \hat{x}E^{n+\frac{1}{2}}_{y_{i,j+\frac{1}{2},ks2}} \end{cases} \tag{25}$$

The electric current densities are defined on the Huygens surface by applying EQ.5 on all the averaged tangential magnetic fields from the secondary grid a half a cell above and below of primary gird surface of the FDTD lattice that coincide with the defined Huygens surface. Taking the average approximately treat the magnetic fields as if they were on the same gird as the electric fields on the primary grid so both the electric and magnetic fields can be defined on the same Huygens surface for consistency. Geometric Averaging will yield better results, but is more computationally expensive, thus in this project only the simple average is applied.The derived electric surface current densities for each of the six faces of the Huygens surface are defined by the normal surface vector labeled is1,js1,ks1,is2,js2,ks2 as illustrated in FIG 2. The electric surface current densities are related to the tangential magnetic fields as given by the relations:

$$\vec{J}is1 \begin{cases} \hat{z}J^{n+\frac{1}{2}}_{z_{is1,j,k+\frac{1}{2}}} = \hat{y}\frac{1}{2}\left(H^{n+\frac{1}{2}}_{y_{is1+\frac{1}{2},j,k+\frac{1}{2}}} + H^{n+\frac{1}{2}}_{y_{is1-\frac{1}{2},j,k+\frac{1}{2}}}\right) \times -\hat{x} = \quad \hat{z}\frac{1}{2}\left(H^{n+\frac{1}{2}}_{y_{is1+\frac{1}{2},j,k+\frac{1}{2}}} + H^{n+\frac{1}{2}}_{y_{is1-\frac{1}{2},j,k+\frac{1}{2}}}\right) \\ \hat{y}J^{n+\frac{1}{2}}_{y_{is1,j+\frac{1}{2},k}} = \hat{z}\frac{1}{2}\left(H^{n+\frac{1}{2}}_{z_{is1+\frac{1}{2},j+\frac{1}{2},k}} + H^{n+\frac{1}{2}}_{z_{is1-\frac{1}{2},j+\frac{1}{2},k}}\right) \times -\hat{x} = -\hat{y}\frac{1}{2}\left(H^{n+\frac{1}{2}}_{z_{is1+\frac{1}{2},j+\frac{1}{2},k}} + H^{n+\frac{1}{2}}_{z_{is1-\frac{1}{2},j+\frac{1}{2},k}}\right) \end{cases} \tag{26}$$

$$\vec{J}js1 \begin{cases} \hat{x}J^{n+\frac{1}{2}}_{x_{i+\frac{1}{2},js1,k}} = \hat{z}\frac{1}{2}\left(H^{n+\frac{1}{2}}_{z_{i+\frac{1}{2},js1+\frac{1}{2},k}} + H^{n+\frac{1}{2}}_{z_{i+\frac{1}{2},js1-\frac{1}{2},k}}\right) \times -\hat{y} = \hat{x}\frac{1}{2}\left(H^{n+\frac{1}{2}}_{z_{i+\frac{1}{2},js1+\frac{1}{2},k}} + H^{n+\frac{1}{2}}_{z_{i+\frac{1}{2},js1-\frac{1}{2},k}}\right) \\ \hat{z}J^{n+\frac{1}{2}}_{z_{i,js1,k+\frac{1}{2}}} = \hat{x}\frac{1}{2}\left(H^{n+\frac{1}{2}}_{x_{i,js1+\frac{1}{2},k+\frac{1}{2}}} + H^{n+\frac{1}{2}}_{x_{i,js1-\frac{1}{2},k+\frac{1}{2}}}\right) \times -\hat{y} = -\hat{z}\frac{1}{2}\left(H^{n+\frac{1}{2}}_{x_{i,js1+\frac{1}{2},k+\frac{1}{2}}} + H^{n+\frac{1}{2}}_{x_{i,js1-\frac{1}{2},k+\frac{1}{2}}}\right) \end{cases} \tag{27}$$

$$\vec{J}ks1 \begin{cases} \hat{y}J^{n+\frac{1}{2}}_{y_{i,j+\frac{1}{2},ks1}} = \hat{x}\frac{1}{2}\left(H^{n+\frac{1}{2}}_{x_{i,j+\frac{1}{2},ks1+\frac{1}{2}}} + H^{n+\frac{1}{2}}_{x_{i,j+\frac{1}{2},ks1-\frac{1}{2}}}\right) \times -\hat{z} = \hat{y}\frac{1}{2}\left(H^{n+\frac{1}{2}}_{x_{i,j+\frac{1}{2},ks1+\frac{1}{2}}} + H^{n+\frac{1}{2}}_{x_{i,j+\frac{1}{2},ks1-\frac{1}{2}}}\right) \\ \hat{x}J^{n+\frac{1}{2}}_{x_{i+\frac{1}{2},j,ks1}} = \hat{y}\frac{1}{2}\left(H^{n+\frac{1}{2}}_{y_{i+\frac{1}{2},j,ks1+\frac{1}{2}}} + H^{n+\frac{1}{2}}_{y_{i+\frac{1}{2},j,ks1-\frac{1}{2}}}\right) \times -\hat{z} = -\hat{x}\frac{1}{2}\left(H^{n+\frac{1}{2}}_{y_{i+\frac{1}{2},j,ks1+\frac{1}{2}}} + H^{n+\frac{1}{2}}_{y_{i+\frac{1}{2},j,ks1-\frac{1}{2}}}\right) \end{cases} \tag{28}$$

$$\vec{J}is2 \begin{cases} \hat{z}J^{n+\frac{1}{2}}_{z_{is2,j,k+\frac{1}{2}}} = \hat{y}\frac{1}{2}\left(H^{n+\frac{1}{2}}_{y_{is2+\frac{1}{2},j,k+\frac{1}{2}}} + H^{n+\frac{1}{2}}_{y_{is2-\frac{1}{2},j,k+\frac{1}{2}}}\right) \times \hat{x} = -\hat{z}\frac{1}{2}\left(H^{n+\frac{1}{2}}_{y_{is2+\frac{1}{2},j,k+\frac{1}{2}}} + H^{n+\frac{1}{2}}_{y_{is2-\frac{1}{2},j,k+\frac{1}{2}}}\right) \\ \hat{y}J^{n+\frac{1}{2}}_{y_{is2,j+\frac{1}{2},k}} = \hat{z}\frac{1}{2}\left(H^{n+\frac{1}{2}}_{z_{is2+\frac{1}{2},j+\frac{1}{2},k}} + H^{n+\frac{1}{2}}_{z_{is2-\frac{1}{2},j+\frac{1}{2},k}}\right) \times \hat{x} = \hat{y}\frac{1}{2}\left(H^{n+\frac{1}{2}}_{z_{is2+\frac{1}{2},j+\frac{1}{2},k}} + H^{n+\frac{1}{2}}_{z_{is2-\frac{1}{2},j+\frac{1}{2},k}}\right) \end{cases} \tag{29}$$

$$\vec{J}js2 \begin{cases} \hat{x}J^{n+\frac{1}{2}}_{x_{i+\frac{1}{2},js2,k}} = \hat{z}\frac{1}{2}\left(H^{n+\frac{1}{2}}_{z_{i+\frac{1}{2},js2+\frac{1}{2},k}} + H^{n+\frac{1}{2}}_{z_{i+\frac{1}{2},js2-\frac{1}{2},k}}\right) \times \hat{y} = -\hat{x}\frac{1}{2}\left(H^{n+\frac{1}{2}}_{z_{i+\frac{1}{2},js2+\frac{1}{2},k}} + H^{n+\frac{1}{2}}_{z_{i+\frac{1}{2},js2-\frac{1}{2},k}}\right) \\ \hat{z}J^{n+\frac{1}{2}}_{z_{i,js2,k+\frac{1}{2}}} = \hat{x}\frac{1}{2}\left(H^{n+\frac{1}{2}}_{x_{i,js2+\frac{1}{2},k+\frac{1}{2}}} + H^{n+\frac{1}{2}}_{x_{i,js2-\frac{1}{2},k+\frac{1}{2}}}\right) \times \hat{y} = \hat{z}\frac{1}{2}\left(H^{n+\frac{1}{2}}_{x_{i,js2+\frac{1}{2},k+\frac{1}{2}}} + H^{n+\frac{1}{2}}_{x_{i,js2-\frac{1}{2},k+\frac{1}{2}}}\right) \end{cases} \tag{30}$$

$$\vec{J}ks2 \begin{cases} \hat{y}J^{n+\frac{1}{2}}_{y_{i,j+\frac{1}{2},ks2}} = \hat{x}\frac{1}{2}\left(H^{n+\frac{1}{2}}_{x_{i,j+\frac{1}{2},ks2+\frac{1}{2}}} + H^{n+\frac{1}{2}}_{x_{i,j+\frac{1}{2},ks2-\frac{1}{2}}}\right) \times \hat{z} = -\hat{y}\frac{1}{2}\left(H^{n+\frac{1}{2}}_{x_{i,j+\frac{1}{2},ks2+\frac{1}{2}}} + H^{n+\frac{1}{2}}_{x_{i,j+\frac{1}{2},ks2-\frac{1}{2}}}\right) \\ \hat{x}J^{n+\frac{1}{2}}_{x_{i+\frac{1}{2},j,ks2}} = \hat{y}\frac{1}{2}\left(H^{n+\frac{1}{2}}_{y_{i+\frac{1}{2},j,ks2+\frac{1}{2}}} + H^{n+\frac{1}{2}}_{y_{i+\frac{1}{2},j,ks2-\frac{1}{2}}}\right) \times \hat{z} = \hat{x}\frac{1}{2}\left(H^{n+\frac{1}{2}}_{y_{i+\frac{1}{2},j,ks2+\frac{1}{2}}} + H^{n+\frac{1}{2}}_{y_{i+\frac{1}{2},j,ks2-\frac{1}{2}}}\right) \end{cases} \tag{31}$$

With the vector components of the magnetic and electric surface currents now defined on the Huygens surface in terms of the tangential electric fields and tangential averaged magnetic fields as expressed by equations (), the vector potential components in spherical coordinates can now be calculated from the discrete versions of equations 16 and 17. The surface currents defined on the Huygens surface are sampled in the time domain since the electric and magnetic fields are calculated in the time domain of the main FDTD routine. To convert

into the frequency domain a running discrete Fourier transform is performed at each time step on the sums over the current densities on the Huygens surface. thus at each time step in the FDTD simulation a new term is added to the running discrete Fourier transform sum. The discrete Fourier transform has to be carried out for every desired frequency the far-fields want to be observed at.

First the L component's of vector potentials will be analyzed. These components correspond to the integration of the magnetic surface currents on the Huygens surface. By grouping the terms of magnetic surface current Mx,My,Mz components (formulated in terms of the tangential electric fields as given by equations 18 through 23) from each face of the Hugyen surface that contributes to the corresponding Lx,ly,lz components and subsequently integrating over the surface with the complex spatial exponential and finally applying discrete Fourier transform sum, the discrete equations are derived for the Lx,Ly,Lz components in the frequency domain:

$$L_x(\theta,\phi) \approx \Delta t \sum_{N=0}^{N} v_0^n e^{-j2\pi f_i (n+\frac{1}{2})\Delta t} \left(\begin{array}{l} \Delta x \Delta y \sum\limits_{j=js1}^{js2-1} \sum\limits_{i=is1}^{is2} v^i_{is1,is2} E^{n+\frac{1}{2}}_{y_{i,j+\frac{1}{2},ks2}} e^{j\vec{k}\cdot\vec{r'}_{i,j+\frac{1}{2},ks2}} - \\ \Delta x \Delta y \sum\limits_{j=js1}^{js2-1} \sum\limits_{i=is1}^{is2} v^i_{is1,is2} E^{n+\frac{1}{2}}_{y_{i,j+\frac{1}{2},ks1}} e^{j\vec{k}\cdot\vec{r'}_{i,j+\frac{1}{2},ks1}} + \\ \Delta x \Delta z \sum\limits_{k=ks1}^{ks2-1} \sum\limits_{i=is1}^{is2} v^i_{is1,is2} E^{n+\frac{1}{2}}_{z_{i,js1,k+\frac{1}{2}}} e^{j\vec{k}\cdot\vec{r'}_{i,js1,k+\frac{1}{2}}} - \\ \Delta x \Delta z \sum\limits_{k=ks1}^{ks2-1} \sum\limits_{i=is1}^{is2} v^i_{is1,is2} E^{n+\frac{1}{2}}_{z_{i,js2,k+\frac{1}{2}}} e^{j\vec{k}\cdot\vec{r'}_{i,js2,k+\frac{1}{2}}} \end{array} \right) \tag{32}$$

$$L_y(\theta,\phi) \approx \Delta t \sum_{N=0}^{N} v_0^n e^{-j2\pi f_i (n+\frac{1}{2})\Delta t} \left(\begin{array}{l} \Delta y \Delta x \sum\limits_{i=is1}^{is2-1} \sum\limits_{j=js1}^{js2} v^j_{js1,js2} E^{n+\frac{1}{2}}_{x_{i+\frac{1}{2},j,ks1}} e^{j\vec{k}\cdot\vec{r'}_{i+\frac{1}{2},j,ks1}} - \\ \Delta y \Delta x \sum\limits_{i=is1}^{is2-1} \sum\limits_{j=js1}^{js2} v^j_{js1,js2} E^{n+\frac{1}{2}}_{x_{i+\frac{1}{2},j,ks2}} e^{j\vec{k}\cdot\vec{r'}_{i+\frac{1}{2},j,ks2}} + \\ \Delta y \Delta z \sum\limits_{k=ks1}^{ks2-1} \sum\limits_{j=js1}^{js2} v^j_{js1,js2} E^{n+\frac{1}{2}}_{z_{is2,j,k+\frac{1}{2}}} e^{j\vec{k}\cdot\vec{r'}_{is2,j,k+\frac{1}{2}}} - \\ \Delta y \Delta z \sum\limits_{k=ks1}^{ks2-1} \sum\limits_{j=js1}^{js2} v^j_{js1,js2} E^{n+\frac{1}{2}}_{z_{is1,j,k+\frac{1}{2}}} e^{j\vec{k}\cdot\vec{r'}_{is1,j,k+\frac{1}{2}}} \end{array} \right) \tag{33}$$

$$L_z(\theta,\phi) \approx \Delta t \sum_{N=0}^{N} v_0^n e^{-j2\pi f_i (n+\frac{1}{2})\Delta t} \left(\begin{array}{l} \Delta z \Delta x \sum\limits_{i=is1}^{is2-1} \sum\limits_{k=ks1}^{ks2} v^k_{ks1,ks2} E^{n+\frac{1}{2}}_{x_{i+\frac{1}{2},js2,k}} e^{j\vec{k}\cdot\vec{r'}_{i+\frac{1}{2},js2,k}} - \\ \Delta z \Delta x \sum\limits_{i=is1}^{is2-1} \sum\limits_{k=ks1}^{ks2} v^k_{ks1,ks2} E^{n+\frac{1}{2}}_{x_{i+\frac{1}{2},js1,k}} e^{j\vec{k}\cdot\vec{r'}_{i+\frac{1}{2},js1,k}} + \\ \Delta z \Delta y \sum\limits_{j=js1}^{js2-1} \sum\limits_{k=ks1}^{ks2} v^k_{ks1,ks2} E^{n+\frac{1}{2}}_{y_{is1,j+\frac{1}{2},k}} e^{j\vec{k}\cdot\vec{r'}_{is1,j+\frac{1}{2},k}} - \\ \Delta z \Delta y \sum\limits_{j=js1}^{js2-1} \sum\limits_{k=ks1}^{ks2} v^k_{ks1,ks2} E^{n+\frac{1}{2}}_{y_{is2,j+\frac{1}{2},k}} e^{j\vec{k}\cdot\vec{r'}_{is2,j+\frac{1}{2},k}} \end{array} \right) \quad (34)$$

Next, the N components of the vector potentials will be analyzed. These components correspond to the integration of the electric surface currents on the averaged Huygens surface. By grouping the terms of electric surface current Jx,Jy,Jz components (formulated in terms of the averaged tangential magnetic fields as given by equations 24 through 29) from each face of the Hugyen surface that contributes to the corresponding Nx,Ny,Nz components and subsequently integrating over the surface with the complex spatial exponential and finally applying discrete Fourier transform sum, the discrete equations are derived for the Nx,Ny,Nz components in the frequency domain:

$$N_x(\theta,\phi) \approx \Delta t \sum_{N=0}^{N} v_0^n e^{-j2\pi f_i (n+\frac{1}{2})\Delta t} \left(\begin{array}{l} \frac{\Delta x \Delta y}{-2} \sum\limits_{j=js1+1}^{js2-1} \sum\limits_{i=is1}^{is2-1} v^i_{is1,is2} \left(H^{n+\frac{1}{2}}_{y_{i+\frac{1}{2},j,ks2+\frac{1}{2}}} + H^{n+\frac{1}{2}}_{y_{i+\frac{1}{2},j,ks2-\frac{1}{2}}} \right) e^{j\vec{k}\cdot\vec{r'}_{i+\frac{1}{2},j,ks2}} + \\ \frac{\Delta x \Delta y}{2} \sum\limits_{j=js1+1}^{js2-1} \sum\limits_{i=is1}^{is2-1} v^i_{is1,is2} \left(H^{n+\frac{1}{2}}_{y_{i+\frac{1}{2},j,ks1+\frac{1}{2}}} + H^{n+\frac{1}{2}}_{y_{i+\frac{1}{2},j,ks1-\frac{1}{2}}} \right) e^{j\vec{k}\cdot\vec{r'}_{i+\frac{1}{2},j,ks1}} - \\ \frac{\Delta x \Delta z}{2} \sum\limits_{k=ks1+1}^{ks-1} \sum\limits_{i=is1}^{is2-1} v^i_{is1,is2} \left(H^{n+\frac{1}{2}}_{z_{i+\frac{1}{2},js1+\frac{1}{2},k}} + H^{n+\frac{1}{2}}_{y_{i+\frac{1}{2},js1-\frac{1}{2},k}} \right) e^{j\vec{k}\cdot\vec{r'}_{i+\frac{1}{2},js1,k}} + \\ \frac{\Delta x \Delta z}{2} \sum\limits_{k=ks1+1}^{ks2-1} \sum\limits_{i=is1}^{is2-1} v^i_{is1,is2} \left(H^{n+\frac{1}{2}}_{z_{i+\frac{1}{2},js2+\frac{1}{2},k}} + H^{n+\frac{1}{2}}_{y_{i+\frac{1}{2},js2-\frac{1}{2},k}} \right) e^{j\vec{k}\cdot\vec{r'}_{i+\frac{1}{2},js2,k}} \end{array} \right) \quad (35)$$

$$N_y(\theta,\phi) \approx \Delta t \sum_{N=0}^{N} v_0^n e^{-j2\pi f_i (n+\frac{1}{2})\Delta t} \left(\begin{array}{l} \frac{\Delta y \Delta x}{-2} \sum\limits_{i=is1-1}^{is2-1} \sum\limits_{j=js1}^{js2-1} v^j_{js1,js2} \left(H^{n+\frac{1}{2}}_{x_{i,j+\frac{1}{2},ks1+\frac{1}{2}}} + H^{n+\frac{1}{2}}_{x_{i,j+\frac{1}{2},ks1-\frac{1}{2}}} \right) e^{j\vec{k}\cdot\vec{r'}_{i,j+\frac{1}{2},ks1}} + \\ \frac{\Delta y \Delta x}{2} \sum\limits_{i=is1-1}^{is2-1} \sum\limits_{j=js1}^{js2-1} v^j_{js1,js2} \left(H^{n+\frac{1}{2}}_{x_{i,j+\frac{1}{2},ks2+\frac{1}{2}}} + H^{n+\frac{1}{2}}_{x_{i,j+\frac{1}{2},ks2-\frac{1}{2}}} \right) e^{j\vec{k}\cdot\vec{r'}_{i,j+\frac{1}{2},ks2}} - \\ \frac{\Delta y \Delta z}{2} \sum\limits_{k=ks1+1}^{ks2-1} \sum\limits_{j=js1}^{js2-1} v^j_{js1,js2} \left(H^{n+\frac{1}{2}}_{z_{is2+\frac{1}{2},j+\frac{1}{2},k}} + H^{n+\frac{1}{2}}_{z_{is2-\frac{1}{2},j+\frac{1}{2},k}} \right) e^{j\vec{k}\cdot\vec{r'}_{is2,j+\frac{1}{2},k}} + \\ \frac{\Delta y \Delta z}{2} \sum\limits_{k=ks1+1}^{ks2-1} \sum\limits_{j=js1}^{js2-1} v^j_{js1,js2} \left(H^{n+\frac{1}{2}}_{z_{is1+\frac{1}{2},j+\frac{1}{2},k}} + H^{n+\frac{1}{2}}_{z_{is1-\frac{1}{2},j+\frac{1}{2},k}} \right) e^{j\vec{k}\cdot\vec{r'}_{is1,j+\frac{1}{2},k}} \end{array} \right) \tag{36}$$

$$N_z(\theta,\phi) \approx \Delta t \sum_{N=0}^{N} v_0^n e^{-j2\pi f_i (n+\frac{1}{2})\Delta t} \left(\begin{array}{l} \frac{\Delta z \Delta x}{-2} \sum\limits_{i=is1-1}^{is2-1} \sum\limits_{k=ks1}^{ks2-1} v^k_{ks1,ks2} \left(H^{n+\frac{1}{2}}_{x_{i,js2+\frac{1}{2},k+\frac{1}{2}}} + H^{n+\frac{1}{2}}_{x_{i,js2-\frac{1}{2},k+\frac{1}{2}}} \right) e^{j\vec{k}\cdot\vec{r'}_{i,js2,k+\frac{1}{2}}} + \\ \frac{\Delta z \Delta x}{2} \sum\limits_{i=is1-1}^{is2-1} \sum\limits_{k=ks1}^{ks2-1} v^k_{ks1,ks2} \left(H^{n+\frac{1}{2}}_{x_{i,js1+\frac{1}{2},k+\frac{1}{2}}} + H^{n+\frac{1}{2}}_{x_{i,js1-\frac{1}{2},k+\frac{1}{2}}} \right) e^{j\vec{k}\cdot\vec{r'}_{i,js1,k+\frac{1}{2}}} - \\ \frac{\Delta z \Delta y}{2} \sum\limits_{k=ks1-1}^{ks2-1} \sum\limits_{k=ks1}^{ks2-1} v^k_{ks1,ks2} \left(H^{n+\frac{1}{2}}_{y_{is1+\frac{1}{2},j,k+\frac{1}{2}}} + H^{n+\frac{1}{2}}_{y_{is1-\frac{1}{2},j,k+\frac{1}{2}}} \right) e^{j\vec{k}\cdot\vec{r'}_{is1,j,k+\frac{1}{2}}} + \\ \frac{\Delta z \Delta y}{2} \sum\limits_{k=ks1-1}^{ks2-1} \sum\limits_{k=ks1}^{ks2-1} v^k_{ks1,ks2} \left(H^{n+\frac{1}{2}}_{y_{is2+\frac{1}{2},j,k+\frac{1}{2}}} + H^{n+\frac{1}{2}}_{y_{is2-\frac{1}{2},j,k+\frac{1}{2}}} \right) e^{j\vec{k}\cdot\vec{r'}_{is2,j,k+\frac{1}{2}}} \end{array} \right) \tag{37}$$

After the time-domain vector potential components are finished computing at the end of the FDTD simulation, the vector potential vector components can be converted from Cartesian to spherical components by the conversion equations:

$$L_\theta = L_x \cos\theta \cos\phi + L_y \cos\theta \sin\phi - L_z \sin\theta \tag{38}$$

$$L_\phi = -L_x \sin\phi + L_y \cos\phi \tag{39}$$

and:

$$N_\theta = N_x \cos\theta \cos\phi + N_y \cos\theta \sin\phi - N_z \sin\theta \tag{40}$$

$$N_\phi = -N_x \sin\phi + N_y \cos\phi. \tag{41}$$

.

Once the fields are converted to spherical components, equations 10-15 can be used to calculate the far fields at the desired radial distance(s) for every Ntheta, Nphi and Ltheta, Lphi computed for every theta, phi and frequency the NFFF was computed at during the

FDTD simulation. With far fields computed, radiation intensities in the far field can be calculated and antenna gain values can be calculated for desired observation points at the various theta, phi angles and frequency values the NFFF was computed for.

III. CODE IMPLEMENTATION

In this section a brief overview of the implementation and top level design of the software that performs the 3D FDTD simulation along with Near-Field to Far-Field Transform are presented. The main FDTD software was provided by Dr. Gedney. The operation of the this code is described by the flowchart of the top level ion figure 5. The areas that are highlighted in this figure represent the areas of the code that were added and modified to implement the NFFF into the MATLAB software.

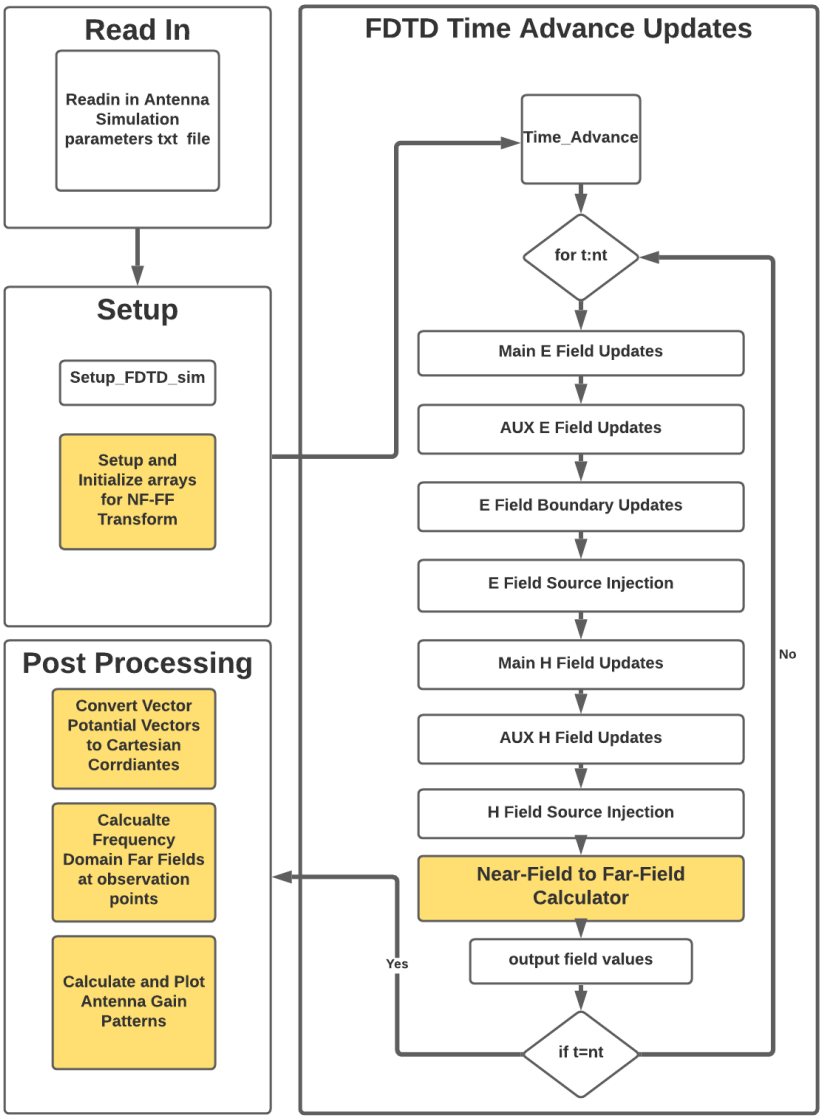

FIG. 3: Block Diagram of the top level design of the FDTD MAT LAB Software made and provided by Dr. Gedney at CU Denver. The highlighted boxes represent the areas of the code where additional code was added to implement a Near-Field to Far-Field Transform.

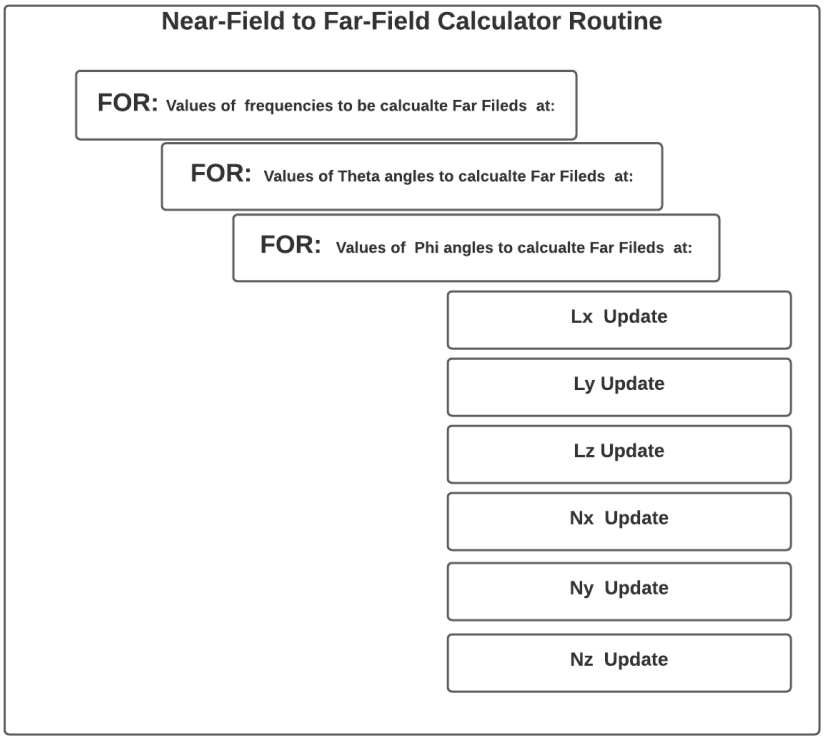

FIG. 4: Block Diagram of the Near-Field to Far-Field Calculator Routine that is performed at each time step in the main FDTD update loop.

IV. VALIDATING CASE STUDIES

In this section, the procedure used to verify the NFFF transform will be described. The firs method to verify the functionality of the NFFF transform was to simulate a simple Hertzian dipole antenna. This is perhaps the simplest antenna to simulate, and the radiation pattern observed should appear in the shape of the torus with the radius spanning around the Axis of the dipole. So far the the NFFF MATLAB code has not passed the verification stage as I have not yet observed the correct radiation pattern of the simple dipole. The incorrect results are still documented however.

A. Hertzian Dipole Validation Test

For the Validation simulation, the FDTDInput.txt file that was provided was used. The parameters in the txt file were changed in order to setup a Hertzian dipole. The Hertzian

dipole was implemented by exciting one electric field edge in the middle of the FDTD space with a current source. The location chosen is labeled by the source coordinates on the primary grid of: $(i^1_{src}, j^1_{src}, k^1_{src}) = (16, 16, 26)$ and $(i^2_{src}, j^2_{src}, k^2_{src}) = (16, 16, 27)$. The near to far field transform was perform for angles of theta between 0 and 360 in 5 degree increments and for angles for phi values between 0 and 360 in 5 degree increments. The NFFF calculations were performed for a observation radial distance of 10 meters and a single frequency of 300 Mhz. The source signature was a differentiated Gaussian pulse with a half pulse width t_w=3.236e-10s. The Huygens surface was positioned in the FDTD space with the coordinate bounds defined by: $(i^1_{src}, j^1_{src}, k^1_{src}) = (14, 14, 24)$ and $(i^2_{src}, j^2_{src}, k^2_{src}) = (18, 18, 29)$ so that the surface is position equally between the PML and the antenna.

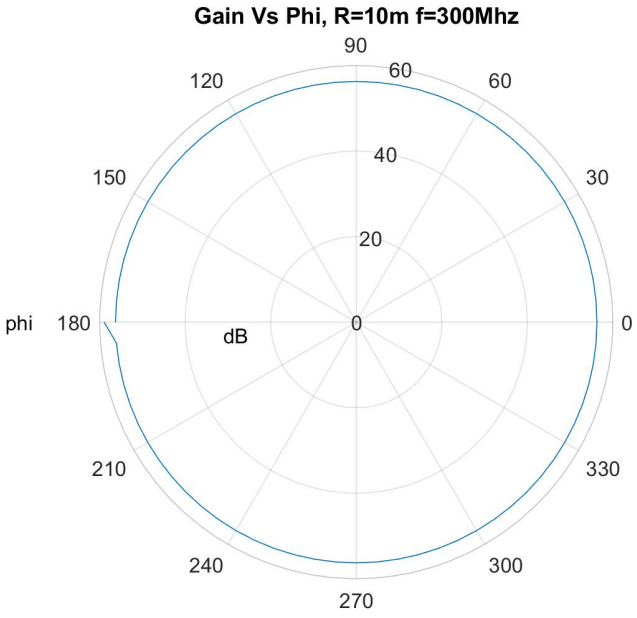

FIG. 5: Polar plot of Gain Vs Phi at a radial distance of 10m and a frequency of 300Mhz of simple Hertzian dipole place in FDTD center

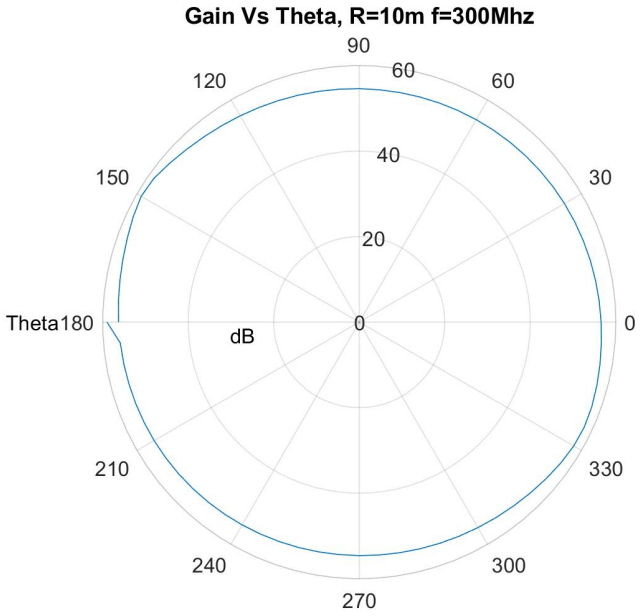

FIG. 6: Polar plot of Gain Vs Theta at a radial distance of 10m and a frequency of 300Mhz of simple Hertzian dipole place in FDTD center

V. SUMMARY

This project was n attempt to make a MATLAB script that performed a Near Field to Far Field transformation . The code was introduced as an additional script file along with modifications to the MATLAB FDTD code provided by Dr. Gedney. The square dipole antenna input file that was provided was used to simulate a simple dipole antenna by changing the source to a current source on one electric field edge in the middle of the FDTD space. The FDTD NFFF simulation output did not demonstrate the results to be expected and more work needs to be done to check the code and also recheck all the numerical equations.

---

[1] Gedney, S. D. (2011). *Introduction to the Finite-Difference Time-Domain (FDTD): Method for Electromagnetics*. San Rafael, CA: Morgan amp; Claypool.

[2] D.J. Robinson and J.B. Schneider, "On the use of the geometric mean in FDTD near-to-far-field transformations," *IEEE Transactions on Antennas and Propagation,* vol. 55,pp. 3204-3211, Nov

2007.